Stability Analysis of an Articulated Agri-Robot Under Different Central Joint Conditions

R. Vidoni, G. Carabin, A. Gasparetto and F. Mazzetto

Abstract In hilly terrains, the exploitation of (semi-)autonomous systems able to travel nimbly and safely on different terrains and perform agricultural operations is still far from reality.

In this perspective, the articulated 4-wheeled system, that shows an optimal steering capacity and the possibility to adapt to uneven terrains thanks to a passive degree of freedom on the central joint, is one of the most promising mobile wheeled-robot architectures. In this work, the instability of this robotic platform is evaluated in the two different conditions, i.e. phase I and phase II [1], and the effect of blocking the passive DoF of the central joint investigated in order to highlight possible stabilizing conditions and best manoeuvring practices for overturning avoidance. In order to do so, a quasi-static model of the robotic platform has been developed and implemented in a Matlab™ simulator thanks to which the different conditions have been studied.

Keywords Articulated-robot · Stability · Agricultural robotics

1 Introduction

Agricultural robotics and autonomous systems for planting, weeding, fruit picking and monitoring have been studied since many years ([2]) and now, smart, cheap and miniaturized sensors and controllers could allow the development of new efficient mechatronic applications that can speed up the race towards the agricultural automation both in the management of field processes ([3]) and in the safety of machines

R. Vidoni(✉) · G. Carabin · F. Mazzetto
Faculty of Science and Technology, Free University of Bozen-Bolzano,
Piazza Universita, 39100 Bolzano, Italy
e-mail: {renato.vidoni,giovanni.carabin,fabrizio.mazzetto}@unibz.it

A. Gasparetto
DIEGM - University of Udine, Via delle Scienze, 33100 Udine, Italy
e-mail: gasparetto@uniud.it

L.P. Reis et al. (eds.), *Robot 2015: Second Iberian Robotics Conference*,
Advances in Intelligent Systems and Computing 417,
DOI: 10.1007/978-3-319-27146-0_26

operating on slopes ([4]; [5]) areas. The latter is strongly related to the configuration of the mobile robot platform, the choice of which is directly dependent on the working environment ([2, 6, 7]).

The vehicle stability is highly affected by the terrain condition and slope ([8]; [9]; [10]) and effective, safe and self-stabilizing systems are still not on-board. Then, mobile terrain platforms for agri-, hilly-, mountain- applications, either human-driven or (semi-)autonomous, are rare.

In [11], it has been highlighted how a versatile robotic platform that could be the solution for easily moving and turning on different slopes and between rows, e.g. vineyards, is the articulated-frame one. Its central joint is made of two (yaw and roll) degrees of freedom (DoFs), one actuated (yaw) to steer and the other passive (roll), to allow the system to adapt to the terrain. It has a smaller external turning radii with respect to vehicles with a conventional configuration [11]. This platform shows two different possible overturning manners ([12]; [1]): the classical stability condition (type II instability) related to the quadrilateral polygon made of the four wheel contacts, and a second critical stability condition created by the passive roll DoF (type I instability). In literature, the Thype I instability has been firstly defined by [12]. In order to study an anti-overturning mechatronic system able to both forecast and prevent critical configurations in a mobile robot, it is very important to model and simulate the system instabilities together with to inverstigate the effect of the passive DoF and its blocking by means of, for example, a mechanical brake.

In this work, the Guzzomi's kinematic and (quasi-)static model has been firstly revised (Sections 2). Then, in Section 3 the instability phases are discussed and, in Sections 4, a Matlab™ emulator and the stability maps for the two different phases computed. Then, in Section 5, the stabilizing effect of the passive DoF blocking has been investigated and evaluated.

2 Model of the Articulated Robot

2.1 Model Assumptions

Under the following basic hypothesis ([1]):

- the roll DoF of the articulated joint is considered frictionless;
- since the robot speed is going to be slow in practical activities, the dynamic effects can be ignored;
- the robot does not slide down the slope, due to a non-limiting coefficient of friction between surface and tyres;
- tyres are considered stiff, so the contact surfaces result in discrete points (not areas);
- the joint mass is negligible, so it does not affect the dynamic behaviour.

the kinematic and quasi-static model can be described.

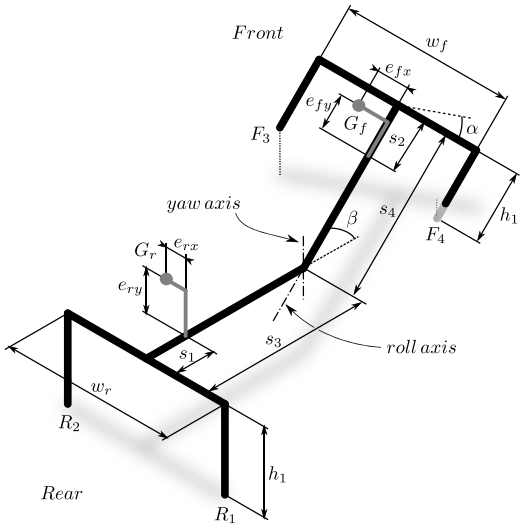

Fig. 1 Kinematic model.

Table 1 Main parameters of the kinematic model.

G_r	CoG of the rear part	e_{rx}	Rear CoG x distance from rear midplane
G_f	CoG of the front part	e_{ry}	Rear CoG y height above roll axis
R_1	Contact point between rear wheel 1 and surface	s_2	Front CoG distance from front axle
R_2	Contact point between rear wheel 2 and surface	e_{fx}	Front CoG x distance from front midplane
F_3	Contact point between front wheel 3 and surface	e_{fy}	Front CoG y height above roll axis
F_4	Contact point between front wheel 4 and surface	w_r	Rear track width
α	Roll angle between rear and front part	w_f	Front track width
β	Yaw angle between rear and front part	h_1	Roll axis height from ground
s_3	Distance from rear axle to central joint	m_r	Rear mass
s_4	Distance from front axle to central joint	m_f	Front mass
s_1	Rear CoG distance from rear axle		

Given the model in Fig. 1, the articulated robot can be explained: a front "f" and a rear "r" parts are connected by a 2 DoF joint which is made of a first revolute DoF, i.e. the yaw β angle, and of a second passive revolute DoF, i.e. the roll α angle. In such a manner the articulated chassis can maintain the four wheels in contact with the substrate even in case of uneven terrains.

In table 1 the geometric parameters of the model shown in Fig. 1 are explained. In order to study the system configurations, the robot is supposed to travel a circle on a sloped surface, which slope ϑ. The robot position related to the maximum slope direction is named φ, β sets the trajectory followed by the robot and α describes the surface conformation ($\alpha = 0$ implies a plane surface), see Fig. 2.

A global coordinate system $(x_0\ y_0\ z_0)$ and two local ones $(x_1\ y_1\ z_1)$ and $(x_2\ y_2\ z_2)$, rigidly attached on the rear and front robot parts respectively, are defined. Then, the matrix $\boldsymbol{R}_1^0$ that describes the rotation from the global system to the rear local one is $\boldsymbol{R}_1^0 = \boldsymbol{R}(\vartheta)\boldsymbol{R}(\varphi)$, i.e. the product of the elementary rotations around the current z and y axis. The rotation matrix $\boldsymbol{R}_2^0$ becomes $\boldsymbol{R}_2^0 = \boldsymbol{R}_1^0\boldsymbol{R}(\beta)\boldsymbol{R}(\alpha)$ with $\boldsymbol{R}(\beta)$ and $\boldsymbol{R}(\alpha)$ elementary rotation matrices around the current y and z axis, respectively.

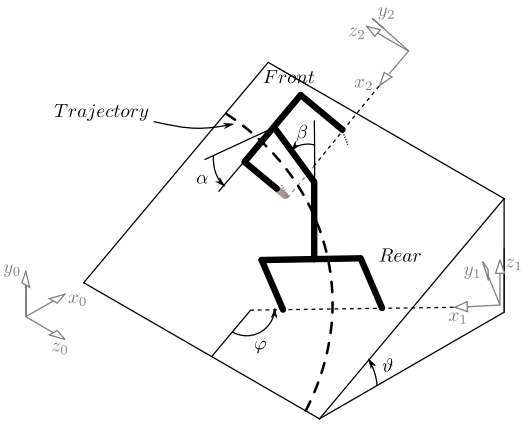

Fig. 2 Robot orientation angles and reference systems.

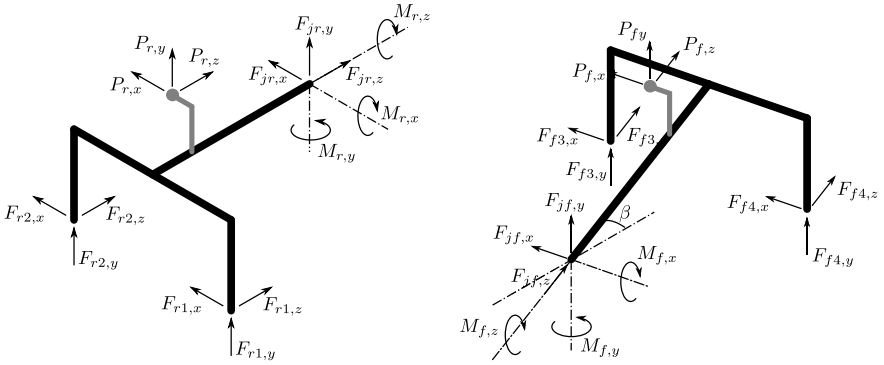

Fig. 3 Dynamic model: (a) rear part, (b) front part.

In order to define and develop a dynamic (quasi-static) model, forces and moments that act on the model have to be evaluated. By referring to Fig. 3, two weight forces $\boldsymbol{P_r}$ and $\boldsymbol{P_f}$, respectively on the rear and front CoG are present. These are counteracted by the four reaction forces $\boldsymbol{F_{r1}}$, $\boldsymbol{F_{r2}}$, $\boldsymbol{F_{f3}}$ and $\boldsymbol{F_{f4}}$, sum of the force normal to the plane and the friction force parallel to the plane. Through the central joint, the forces ($\boldsymbol{F_{jr}}$ and $\boldsymbol{F_{jf}}$) and moments ($\boldsymbol{M_r}$ e $\boldsymbol{M_f}$) are exchanged. The two weight forces $\boldsymbol{P_r}$ and $\boldsymbol{P_f}$, and, due to the absence of friction, the moment $M_{f,z}$ are known.

Since the four normal forces $F_{r1,y}$, $F_{r2,y}$, $F_{f3,y}$ and $F_{f4,y}$ acting on the wheels are needed to study the stability, it is desirable to reduce the system dimension to improve the computational speed with respect to solve the whole system made of 23 equations. By considering the relations of forces and torques in the joint and the fact that all the forces $\boldsymbol{F_{r1}}$, $\boldsymbol{F_{r2}}$, $\boldsymbol{F_{f3}}$ and $\boldsymbol{F_{f4}}$ have a vertical direction with respect to the global reference system, with some reformulations the system can be simplified and, from the initial 23 unknowns, reduced to only 6: F_{r1}, F_{r2}, F_{f3}, F_{f4}, $M_{f,x}$ and $M_{f,y}$.

In such a manner, six equilibrium equations can be written:

$$F_{r1} + F_{r2} + F_{f3} + F_{f4} = P_r + P_f \tag{1}$$

$$M_{f,x} = F_{f3}\left(k_{fy}s_4 + k_{fz}h_1\right) + F_{f4}\left(k_{fy}s_4 + k_{fz}h_1\right) + P_f\left[k_{fy}\left(s_4 - s_2\right) - k_{fz}e_{fy}\right] \tag{2}$$

$$M_{f,y} = F_{f3}\left(-k_{fx}s_4 + k_{fz}\frac{w_f}{2}\right) + F_{f4}\left(-k_{fx}s_4 - k_{fz}\frac{w_f}{2}\right) + P_f\left[-k_{fx}\left(s_4 - s_2\right) + k_{fz}e_{fx}\right] \tag{3}$$

$$M_{f,z} = F_{f3}\left(-k_{fx}h_1 - k_{fy}\frac{w_f}{2}\right) + F_{f4}\left(-k_{fx}h_1 + k_{fy}\frac{w_f}{2}\right) + P_f\left(k_{fx}e_{fy} - k_{fy}e_{fx}\right) = 0 \tag{4}$$

$$\begin{aligned} M_{r,x} &= -\cos\alpha\cos\beta\, M_{f,x} + \sin\alpha\cos\beta\, M_{f,y} \\ &= F_{r1}\left(-k_{ry}s_3 + k_{rz}h_1\right) + F_{r2}\left(-k_{ry}s_3 + k_{rz}h_1\right) + P_r\left[-k_{ry}\left(s_3 - s_1\right) - k_{rz}e_{ry}\right] \end{aligned} \tag{5}$$

$$\begin{aligned} M_{r,z} &= \cos\alpha\sin\beta\, M_{f,x} - \sin\alpha\sin\beta\, M_{f,y} \\ &= F_{r1}\left(-k_{rx}h_1 + k_{ry}\frac{w_r}{2}\right) + F_{r2}\left(-k_{rx}h_1 - k_{ry}\frac{w_r}{2}\right) + P_r\left(k_{rx}e_{ry} - k_{ry}e_{rx}\right) \end{aligned} \tag{6}$$

in the 6 unknowns F_{r1}, F_{r2}, F_{f3}, F_{f4}, $M_{f,x}$ and $M_{f,y}$.

3 Instability Phases

The instability of an articulated robot can be subdivided in phase I and II ([12] and [1]). By increasing the slope (in a quasi-static condition), the force distribution on the four wheels changes according to the configuration and system properties. The articulated system is stable until one of the four reaction forces falls to zero. After that, the roll moment equilibrium is not satisfied, one wheel loses the contact and one part of the robot starts to roll, i.e. the phase I instability occurs. To detect the phase I instability limit condition, the system of six equations has to be solved for every configuration in terms of slope (ϑ angle), robot placement (φ angle), robot trajectory (β angle) and terrain conformation (α angle).

The phase I instability creates a roll motion in a part of the robot. This motion stops when the joint reaches its mechanical limit (also a brake can stop the motion in an intermediate position) and the robot chassis becomes a unique rigid body. In this condition the instability occurs only when the CoG projection point falls out from the equilibrium polygon made of the wheel contact points, i.e. the phase II instability.

4 Numerical Implementation

The overall stability model has been implemented in a Matlab™ environment. Its outputs are a matrix with the stability limits and an instability map where, for a given robot configuration, i.e. α and β angles, the following information are shown:

– plane slope limits for phase I instability ($\vartheta_{lim,I}$);
– tyre that looses the contact with the terrain in phase I instability;

Table 2 Robot emulator geometric and physical parameters.

s_1 [mm]	s_2 [mm]	s_3 [mm]	s_4 [mm]	w_r [mm]	w_f [mm]	h_1 [mm]	e_{rx} [mm]	e_{fx} [mm]	e_{ry} [mm]	e_{fy} [mm]	m_r [kg]	m_f [kg]
26	55	200	200	240	180	94	0	0	20	14	1,34	1,84

– plane slope limits for phase II instability ($\vartheta_{lim,II}$);
– angular margin $\Delta\vartheta = \vartheta_{lim,II} - \vartheta_{lim,I}$, that will be gained if the joint is blocked.

The simulator finds the solution by an iterative algorithm based on the bisection method, one for the phase I and one for the phase II instability. In that manner, by the superimposition of the two instabilities limits, it is possible to evaluate the possible stability enhancement of the joint's passive DoF blocking. Thus, the idea is to evaluate the stabilizing effect of a blocking action when approaching the phase I instability and find out some directives and "best driving practices" for the articulated robotic platform. In table 2, the simulated robot parameters referred to a real emulator, see figure 4, are listed.

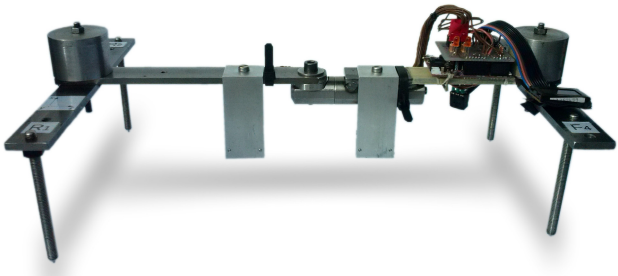

Fig. 4 Emulator of the articulated robotic platform.

5 Simulations and Results

The stability map is the main output of the Matlab simulator and the first considered case is the one of a robot travelling along a straight line ($\beta = 0°$) and a terrain with a regular surface ($\alpha = 0°$), figure 5.

The phase I instability curve is always below the phase II curve, except for some φ values in which they are overlapped. So, unless of these points, the strategy of blocking the passive roll DoF would guarantee an extra margin to the robot instability. More in details, this $\Delta\vartheta$ safety angular margin changes with φ and presents local maxima when φ is about 60, 120, 244 and 295° (i.e. when the robot goes uphill or descends with an oblique trajectory). It has to be underlined how these maxima correspond to $\vartheta_{lim,I}$ values that are high; this means that, in this case, the configurations where the blocking action could give the greatest stabilizing effect are when

the slope condition is very critical. However, if the phase I minima are evaluated, i.e. φ equal to 0 and 180°, is it possible to achieve an extra slope margin of about 4°. In particular, practical conditions where φ goes from 0° to 75°, the extra slope margin is always over 4°. There is no extra slope margin for φ equal to 95°, 228°, 270°, and 310°, due to overlapping of phase I and phase II instability curves.

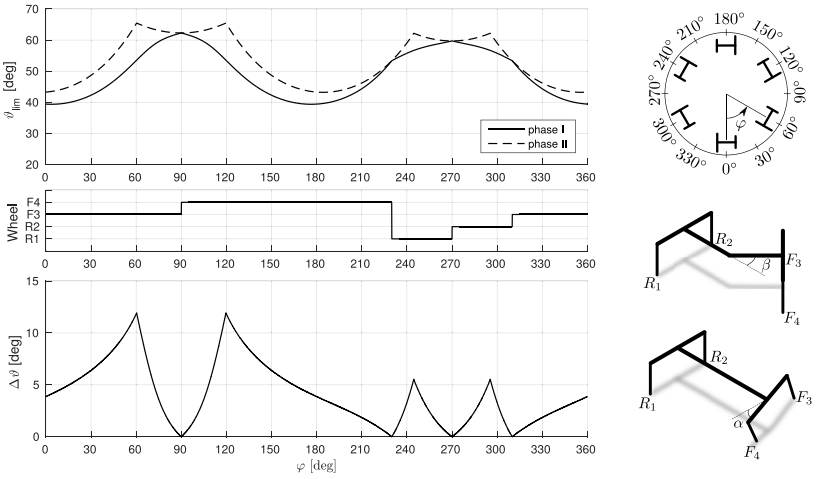

Fig. 5 Stability map related to $\beta = 0°$ and $\alpha = 0°$.

The considered case, in which the robot travels sideways the slope ($\varphi = 0°$ and $\varphi = 180°$), is one of the most critical and common practical cases. However, it is extremely important to consider the possible stabilizing effect if also the β and α angles change, e.g. when the robotic system goes out to a row of wines in a hill and starts turning up in order to go in to the next one or with an uneven sloped terrain.

In figures 6 and 7, the stability map for a regular surface terrain ($\alpha = 0°$) and two robot steering cases, i.e. upstream turning with $\beta = 20°$ and $\beta = 45°$ are presented while in figure 8 the phase I limits for the three different cases are shown.

It can be seen how, the variation of the turning angle β influences both the minimum value of the instability slope angle and its map position along the φ axis: if β increases (upstream turning), the minimum moves from $\varphi = 0°$ to a lower value, and decreases its magnitude; in the downstream turning condition, i.e. $\varphi > 180°$, the contrary occurs.

By considering uneven terrains, i.e. $\alpha \neq 0°$, other important considerations can be made. Figure 9 shows the phase I stability angle for $\beta = 0°$ and considering three different α values. In this case, α influences only the magnitude of the local minima, and not its position along φ axis.

Now, looking at the case in which $\varphi = 0°$ (similar to $\varphi = 180°$ due to the fact that the two COGs locations are almost on the midplane), the correlation between the

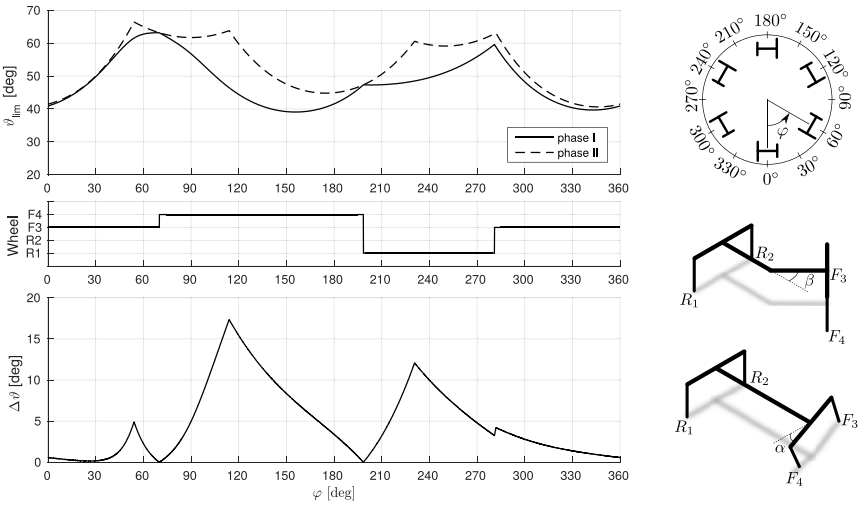

Fig. 6 Stability map related to $\beta = 20°$ and $\alpha = 0°$.

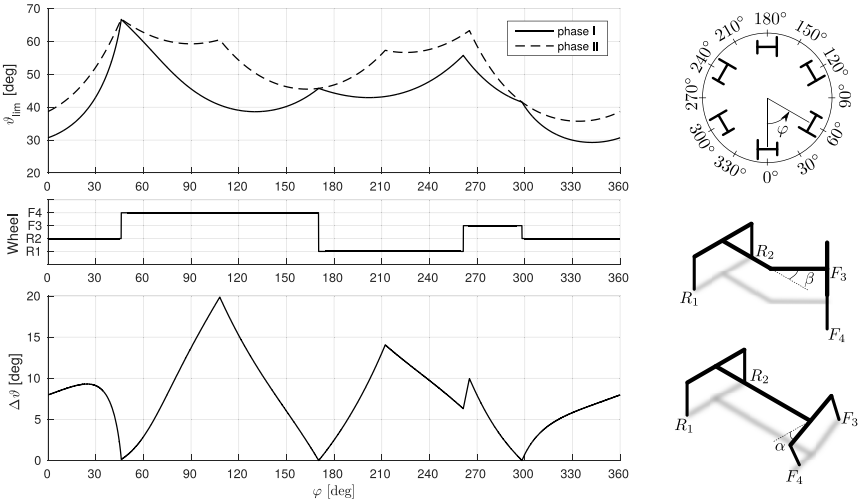

Fig. 7 Stability map related to $\beta = 45°$ and $\alpha = 0°$.

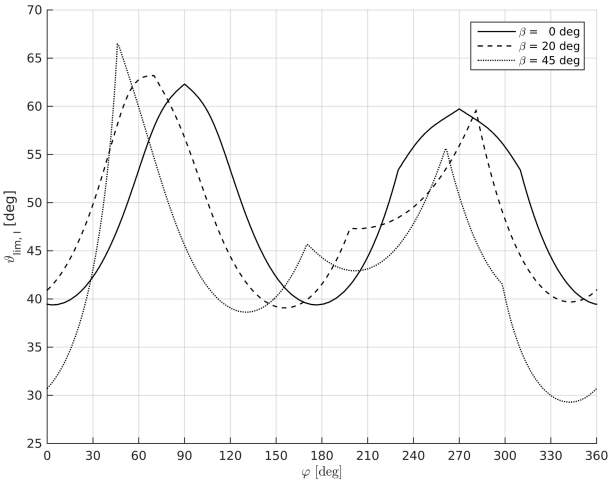

Fig. 8 Stability map for different robot turn levels (β angle), and $\alpha = 0°$.

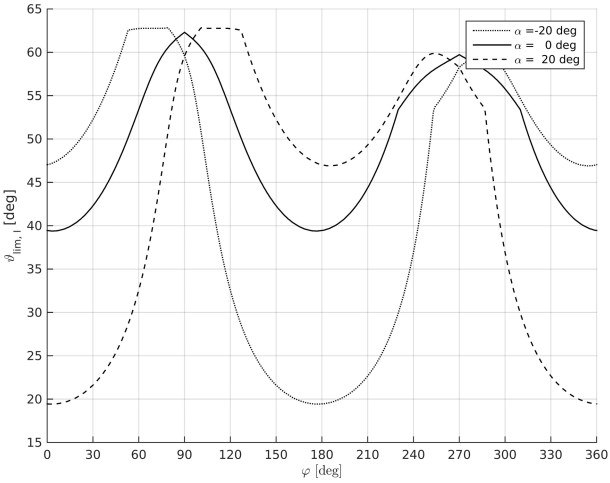

Fig. 9 Stability map for different surface conformation (α angle), and $\beta = 0°$.

angle β and the stability is shown in figure 10. If the robot is in a stable condition with $\beta = 0°$ and starts turning downstream (negative values of β), the phase I stability angle increases; so it should not be necessary to activate the joint brake, since the robot would already be in a stable condition. On the contrary, if the robot starts turning upstream, the phase I stability value increases until a maximum point and, after that,

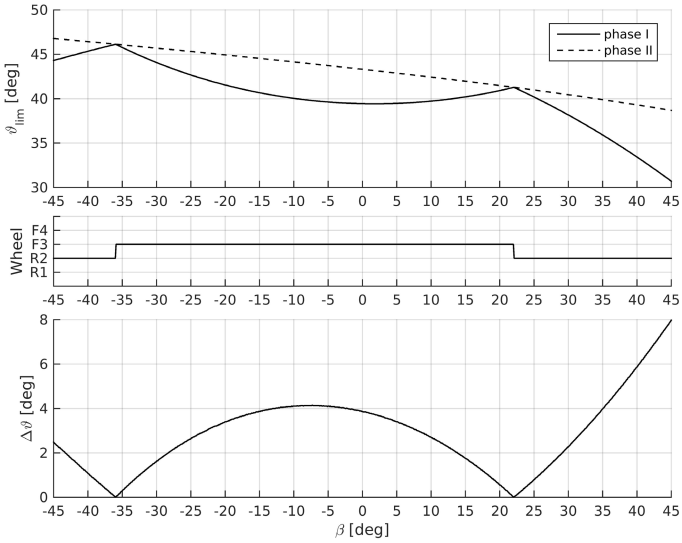

Fig. 10 Stability vs β angle, at $\varphi = 0°$ and $\alpha = 0°$.

it fast decreases. In the first turning phase, blocking the joint would not be necessary due to the positive curve slope; indeed, by increasing the turning angle, increases also the stability. After the point of maximum, it would be necessary (negative curve slope) to block the passive DoF in order to increase the stability.

There is another motivation to block the joint between the interval $\beta = [0, 24]°$, i.e. upstream motion up to the stability curve slope changing: if the robot is near to an unstable condition and β is inner this interval and the operator wants to move in a safer condition, he instinctively reduces the steering angle by a counter-steering manoeuvre. In this way, the robot tends to roll-over, since in this range the phase I instability angle limit decreases with β. Otherwise, with the passive DoF blocked, it does not occur, i.e. the curve slope is negative.

In figure 11 the case of $\varphi = 0°$ and $\beta = 0°$ is considered. When α has positive values, i.e. the robot front part is in a more sloped condition than the rear one, both the phase I and II stability limit angles decrease. However, the phase II angle shows a lower slope, thus blocking the passive DoF would give the possibility to gain an extra angular margin. On the contrary, when α is negative both the phase I and II stability limit angles increase up to the value of $-8°$. After that, the phase I stability limit angle remains constant due to the fact that the phase I instability critical condition goes to the robot rear part, while the phase II instability limit angle still increases thus allowing a more stable condition if the passive DoF is blocked.

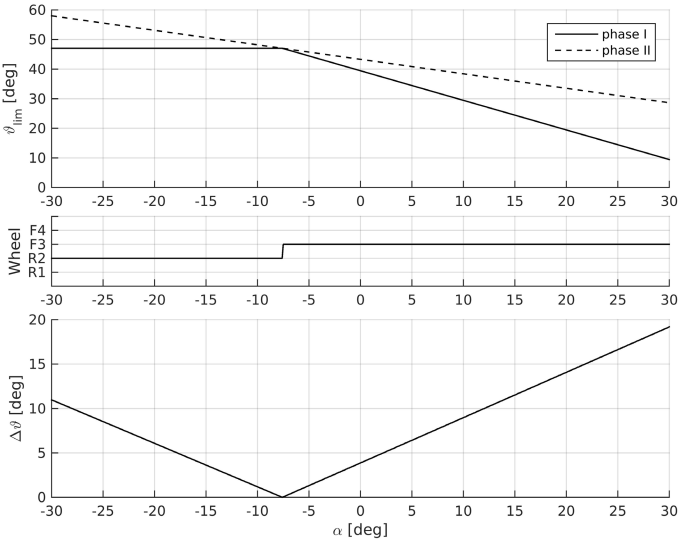

Fig. 11 Stability vs α angle, at $\varphi = 0°$ and $\beta = 0°$.

6 Conclusions

In this work, an articulated 4-wheeled robotic platform suitable for side-slope agricultural activities has been evaluated in its stability conditions. First of all the kinematic and (quasi-)static model has been revised and the two different instability conditions, i.e. phase I and phase II, evaluated. These results have been implemented in a Matlab simulator which gives as output the stability maps and roll-over limits. Then, by considering the fact that this platform shows an optimal steering capacity and the possibility to adapt to uneven terrains thanks to a passive degree of freedom on its central joint, the most critical conditions have been investigated. By focusing on the possibility to block the passive DoF of the central joint, its possible stabilizing effect and best manoeuvring practices for overturning avoidance have been studied and highlighted. Future work will cover experimental tests on a real robotic prototype and/or articulated tractor.

References

1. Baker, V., Guzzomi, A.L.: A model and comparison of 4-wheel-drive fixed-chassis tractor rollover during phase I. Biosystems Engineering **116**(2), 179–189 (2013)
2. Billingsley, J., Visala, A., Dunn, M.: Robotics in agriculture and forestry. In: Siciliano, B., Khatib, O. (eds.) Springer Handbook of Robotics, pp. 1064–1077 (2008)

3. Fumagalli, M., Acutis, M., Mazzetto, F., Vidotto, F., Sali, G., Bechini, L.: A methodology for designing and evaluating alternative cropping systems: application on dairy and arable farms. Ecological Indicators **23**, 189–201 (2012)
4. Khot, L.R., Tang, L., Steward, B.L., Han, S.: Sensor fusion for improving the estimation of roll and pitch for an agricultural sprayer. Biosystems Engineering **101**(1), 13–20 (2008)
5. Kise, M., Zhang, Q.: Sensor-in-the-loop tractor stability control: look-ahead attitude prediction and field tests. Computers and Electronics in Agricultur **52**(1–2), 107–118 (2006)
6. Lee, J.-H., Park, J.B., Lee, B.H.: Turnover prevention of a mobile robot on uneven terrain using the concept of stability space. Robotica **27**(5), 641–652 (2009)
7. Agheli, M., Nestinger, S.: Study of the foot force stability margin for multilegged/wheeled robots under dynamic situations. In: Proceedings of the 8th IEEE/ASME International Conference on Mechatronics and Embedded Systems and Applications, pp. 99–104 (2012)
8. Gravalos, I., Gialamas, T., Loutridis, S., Moshou, D., Kateris, D., Xyradakis, P., Tsiropoulos, Z.: An experimental study on the impact of the rear track width on the stability of agricultural tractors using a test bench. Journal of Terramechanics **48**(4), 319–323 (2011)
9. Mazzetto, F., Bietresato, M., Vidoni, R.: Development of a dynamic stability simulator for articulated and conventional tractors useful for real-time safety devices. Applied Mechanics and Materials **394**, 546–553 (2013)
10. Previati, G., Gobbi, M., Mastinu, G.: Mathematical models for farm tractor rollover prediction. International Journal of Vehicle Design **64**(2–3–4), 280–303 (2014)
11. Vidoni, R., Bietresato, M., Gasparetto, A., Mazzetto, F.: Evaluation and stability comparison of different vehicle configurations for robotic agricultural operations on side-slopes. Biosystems Engineering **129**, 197–211 (2015)
12. Guzzomi, A.L.: A revised kineto-static model for phase I tractor rollover. Biosystems Engineering **113**(1), 65–75 (2012)